BJP British Journal of Pharmacology

DOI:10.1111/j.1476-5381.2012.01958.x
www.brjpharmacol.org

RESEARCH PAPER

Mitochondrial F_0F_1-ATP synthase is a molecular target of 3-iodothyronamine, an endogenous metabolite of thyroid hormone

S Cumero[1], F Fogolari[1], R Domenis[1], R Zucchi[3], I Mavelli[1,2] and S Contessi[1]

[1]*Department of Medical and Biological Sciences, MATI Centre of Excellence, University of Udine, Udine, Italy,* [2]*INBB Istituto Nazionale Biostrutture e Biosistemi, Rome, Italy, and* [3]*Dipartimento di Scienze dell'Uomo e dell'Ambiente, University of Pisa, Pisa, Italy*

Correspondence
Irene Mavelli, Department of Medical and Biological Sciences, University of Udine, P.le Kolbe 4, 33100 Udine, Italy. E-mail: irene.mavelli@uniud.it

Keywords
3-iodothyronamine (T1AM); F_0F_1-ATP synthase; F_1-ATPase; IF_1; aurovertin B; resveratrol; multiple inhibition kinetics; molecular docking analysis

Received
17 January 2011
Revised
21 December 2011
Accepted
29 February 2012

BACKGROUND AND PURPOSE

3-iodothyronamine (T1AM) is a metabolite of thyroid hormone acting as a signalling molecule via non-genomic effectors and can reach intracellular targets. Because of the importance of mitochondrial F_0F_1-ATP synthase as a drug target, here we evaluated interactions of T1AM with this enzyme.

EXPERIMENTAL APPROACH

Kinetic analyses were performed on F_0F_1-ATP synthase in sub-mitochondrial particles and soluble F_1-ATPase. Activity assays and immunodetection of the inhibitor protein IF_1 were used and combined with molecular docking analyses. Effects of T1AM on H9c2 cardiomyocytes were measured by *in situ* respirometric analysis.

KEY RESULTS

T1AM was a non-competitive inhibitor of F_0F_1-ATP synthase whose binding was mutually exclusive with that of the inhibitors IF_1 and aurovertin B. Both kinetic and docking analyses were consistent with two different binding sites for T1AM. At low nanomolar concentrations, T1AM bound to a high-affinity region most likely located within the IF_1 binding site, causing IF_1 release. At higher concentrations, T1AM bound to a low affinity-region probably located within the aurovertin binding cavity and inhibited enzyme activity. Low nanomolar concentrations of T1AM increased ADP-stimulated mitochondrial respiration in cardiomyocytes, indicating activation of F_0F_1-ATP synthase consistent with displacement of endogenous IF_1,, reinforcing the *in vitro* results.

CONCLUSIONS AND IMPLICATIONS

Effects of T1AM on F_0F_1-ATP synthase were twofold: IF_1 displacement and enzyme inhibition. By targeting F_0F_1-ATP synthase within mitochondria, T1AM might affect cell bioenergetics with a positive effect on mitochondrial energy production at low, endogenous, concentrations. T1AM putative binding locations overlapping with IF_1 and aurovertin binding sites are described.

Abbreviations

$\Delta\mu H^+$, proton motive force; ASp, AS particles;; IF_1, F_0F_1-ATP synthase inhibitor protein; K_i inhibition constant; SMP, Mg-ATP sub-mitochondrial particles; T1AM, 3-iodothyronamine

Introduction

3-iodothyronamine (T1AM) is a recently discovered metabolite of thyroid hormone that is thought to derive from thyroxine as a result of enzymatic deiodination and decarboxylation (Scanlan *et al.*, 2004; Zucchi *et al.*, 2010). It has been proposed to act via non-genomic effectors as a signalling molecule that can rapidly influence several physiological manifestations of thyroid hormone action, including thermal homeostasis (Scanlan *et al.*, 2004), fuel metabolism (Braulke *et al.*, 2008), hormone secretion (Regard *et al.*, 2007; Klieverik *et al.*, 2009) and neuronal function (Snead *et al.*, 2007). Administration of exogenous T1AM *in vivo* at micromolar concentrations produces immediate bradycardia and reduced cardiac output, thereby providing evidence of a new aminergic system that modulates cardiac function (Chiellini *et al.*, 2007). In addition, in isolated hearts, T1AM decreased cardiac contractility and increased the resistance to ischemic injury. Contractile effects have been attributed to reduced sarcoplasmic reticulum calcium release (Ghelardoni *et al.*, 2009). Cardioprotection occurs at T1AM concentrations which are much lower than those able to affect contractile function and it has been not associated with any evidence of altered calcium homeostasis, while pharmacological evidence suggests a potential role of mitochondrial effects (Frascarelli *et al.*, 2011), although the detailed mechanisms remain to be elucidated.

Endogenously produced T1AM has been detected *in vivo* at nanomolar concentrations in several rat tissues, in mouse brain, as well as in human, rat, mouse and guinea pig blood (Saba *et al.*, 2010). T1AM interacts with the trace amine-associated receptor 1 (TAA_1), a member of a novel family of membrane G-protein coupled receptors (GPCRs) (Zucchi *et al.*, 2006; Grandy, 2007; receptor nomenclature follows Alexander *et al.*, 2011). The action of T1AM at extracellularly accessible targets, such as TAA_1, is terminated by its uptake into cells, which involves multiple transporters that control the intracellular distribution of the compound (Ianculescu *et al.*, 2009). This transport gives T1AM access to potential intracellular targets, such as the vesicular monoamine transporter VMAT2 (Snead *et al.*, 2007) and mitochondrial proteins (Frascarelli *et al.*, 2011; Venditti *et al.*, 2011). Therefore, identifying additional intracellular targets of T1AM may have physiological and pharmacological importance.

F_0F_1-ATP synthase is a multi-subunit, membrane-associated protein complex that catalyses the phosphorylation of ADP to ATP at the expense of a proton-motive force generated by an electron transport chain in energy-transducing membranes (Boyer, 1997; Stock *et al.*, 2000; Pedersen, 2007; Watt *et al.*, 2010). The mitochondrial enzyme comprises a globular F_1 catalytic domain (subunit composition: $\alpha_3\beta_3\gamma\delta\varepsilon$), termed F_1-ATPase when isolated, and a membrane-bound F_0 proton translocating domain, linked together by central (Gibbons *et al.*, 2000) and peripheral stalks (Dickson *et al.*, 2006; Rees *et al.*, 2009).

The crystal structures of F_1-ATPase demonstrate that the α and β subunits of the F_1 domain are structurally similar, and each subunit consists of three domains: a small N-terminal domain, a nucleotide binding domain and a helical C-terminal domain (Abrahams *et al.*, 1994; Capaldi and Aggeler, 2002; Leyva *et al.*, 2003). Both α and β subunits bind nucleotides, but only the β subunit participates in catalysis. Because of the asymmetry of the γ-subunit, the catalytic β-subunits adopt different conformations with different nucleotide occupancies. Two of the β-subunits are designated β_{DP} and β_{TP}, while the third has no bound nucleotide and is thus referred to as 'empty' and designated β_E (Abrahams *et al.*, 1994). The structures of F_1-ATPase provided insight into the binding change mechanism: the interconversion of the different β-subunit conformations was proposed to occur during the catalytic cycle due to rotation of the central stalk (Abrahams *et al.*, 1994; Capaldi and Aggeler, 2002; Leyva *et al.*, 2003).

The activity of F_0F_1-ATP synthase is regulated by ADP, the proton motive force ($\Delta\mu H^+$) and by its natural inhibitor protein, IF_1 (Harris and Das, 1991) – a basic amphiphilic protein of 84 amino acids (Green and Grover, 2000) that acts as a non-competitive inhibitor by binding to the F_1 domain with a 1:1 stoichiometry. Binding is regulated by physiological levels of ATP, Ca^{2+} and Mg^{2+} (Hong and Pedersen, 2008; Johnson and Ogbi, 2011). Moreover, low pH and $\Delta\mu H^+$ (Lippe *et al.*, 1988), and the hydrolysis of Mg-ATP (Rouslin, 1983) promote the formation of the inhibited IF_1–F_1 complex, while higher pH and $\Delta\mu H^+$ displaces IF_1 from its inhibitory site (Hassinen *et al.*, 1998). As resolved from high-resolution crystallography, IF_1 binds to a site at the catalytic interface between the C-terminal domains of the α_{DP}- and β_{DP}-subunits (Cabezon *et al.*, 2003; Bason *et al.*, 2011), and it detaches from this site upon enzyme rotation and conversion of the *β* subunits during ATP synthesis (Gledhill *et al.*, 2007b). IF_1-mediated inhibition is widely accepted to be essential during myocardial ischemia, when F_0F_1-ATP synthase switches from ATP synthesis to ATP hydrolysis (Rouslin, 1983; Harris and Das, 1991), as well as in ischaemic and pharmacological preconditioning (Contessi *et al.*, 2004; Grover *et al.*, 2006; Comelli *et al.*, 2007). More recent data indicate that IF_1 can regulate mitochondrial F_0F_1-ATP synthase function and supra-molecular organization under both physiological and pathological conditions (García *et al.*, 2006; Campanella *et al.*, 2008), and that variations in IF_1 expression level may play a significant role in defining resting rates of ROS generation and in regulating autophagy (Campanella *et al.*, 2009; Hall *et al.*, 2009). Discovery of additional natural factors able to affect the IF_1 steady-state binding to F_0F_1-ATP synthase may contribute to highlight such processes.

Several covalent and non-covalent inhibitors of mitochondrial F_1-ATPase have been identified and the study of their kinetics, together with the biophysical localization of their binding sites, has helped to clarify the catalytic mechanism of the enzyme. In addition to the IF_1 binding site mentioned above (Gledhill *et al.*, 2007b), high-resolution crystallography has led to the identification of four inhibitory sites: the polyphenolic phytochemicals site, the catalytic site, the aurovertin site and the efrapeptin binding site (Abrahams *et al.*, 1994; van Raaij *et al.*, 1996; Menz *et al.*, 2001; Kagawa *et al.*, 2004; Gledhill *et al.*, 2007a). Depending on experimental conditions, the antibiotic aurovertin has been found to exert uncompetitive, non-competitive or partial mixed inhibition of both ATP hydrolysis and synthesis (Johnson *et al.*, 2009), while the polyphenolic inhibitors, piceatannol and

resveratrol, exhibit non-competitive and mixed inhibition respectively (Bullough *et al.*, 1989; Zheng and Ramirez, 1999; 2000).

Over recent years, F_0F_1-ATP synthase has been highlighted as a molecular target for drugs aimed at the regulation of energy metabolism and the treatment of various diseases, such as autoimmune and immune disorders (Hong and Pedersen, 2008; Johnson and Ogbi, 2011). In this field, some benzodiazepine-based inhibitors of F_0F_1-ATP synthase (BMS compounds) selectively inhibit ATP hydrolase activity and the ATP decline during ischemia, while not affecting ATP production in normoxic and reperfused hearts (Grover and Malm, 2008). Moreover, the presence of F_0F_1-ATP synthase on the surface of several animal cell types has been suggested, indicating that the enzyme is linked to multiple cell processes, including lipid metabolism, intracellular pH regulation, angiogenesis and programmed cell death (see Champagne *et al.*, 2006). F_0F_1-ATP synthase is also a target of antimicrobial agents; for example in *Mycobacterium*, two mutations in its c-subunit confer resistance to the new anti-tuberculosis drug diarylquinoline (Cole and Alzari, 2005). Thus, the development of new F_0F_1-ATP synthase-directed agents has been encouraged.

The aim of the present work was to investigate whether T1AM interacts with F_0F_1-ATP synthase, and to characterize the effects of such an interaction upon enzyme activity taking advantage of kinetic and crystallographic data of natural dietary stilbene polyphenolic compounds and aurovertin B. To do so, kinetic analyses of the interaction of T1AM with F_0F_1-ATP synthase in bovine heart mitochondrial membranes and F_1-ATPase in solution were combined with the modelling of F_1-ATPase structures, leading to the generation of a model of T1AM binding locations on the F_1 domain and the elucidation of the T1AM mechanism of action. We suggest that T1AM may target F_0F_1-ATP synthase within mitochondria, as confirmed when applied to heart-derived cells, and elicit a twofold effect on the enzyme (IF_1 displacement and activity inhibition), thereby affecting cell bioenergetics.

Methods

Sub-mitochondrial particle preparation

Heavy-layer mitochondria from bovine hearts (obtained from an abattoir) were prepared in the absence or presence of succinate and were used to prepare type I and type II MgATP sub-mitochondrial particles (SMP) respectively (Ferguson *et al.*, 1977). AS particles (ASp) were obtained by removing IF_1 from heavy-layer bovine heart mitochondria by high pH treatment followed by gel filtration chromatography (Vadineanu *et al.*, 1976). All particle preparations were stored at –80°C for later use.

As previously reported (Ferguson *et al.*, 1977), type I SMP (containing IF_1-rich F_0F_1-ATP synthase) showed a specific ATPase activity of 2.5 ± 0.3 U·mg^{-1}, while type II SMP (depleted of IF_1) showed a greater activity, 5 ± 0.2 U·mg^{-1}. ASp showed the highest value of ATPase activity, 13 ± 0.4 U·mg^{-1}.

Particle protein concentration was assayed using the Lowry method (Lowry *et al.*, 1951) with BSA as standard.

Purification and preparation of proteins

The soluble F_1 sector of F_0F_1-ATP synthase (F_1-ATPase) was isolated from bovine heart mitochondria as described by Horstman and Racker (1970) then passed through an XK16/40 Superdex 200pg column equilibrated with 20 mM Tris/HCl pH 8.5, 200 mM NaCl, 1 mM ATP, 1 mM EDTA and 5 mM 2-mercaptoethanol buffer according to Abrahams *et al.* (1994). IF_1 was purified from the same source as reported in Gomez-Fernandez and Harris (1978). The purity of the preparations was analysed by SDS-PAGE (see Laemmli, 1970). Concentrations of F_1-ATPase and IF_1 protein were assayed by the bicinchoninic acid method described by Smith *et al.* (1985) with BSA as standard.

Inhibition assay

F_0F_1-ATP synthase activity was measured after incubation with various concentrations (0–90 μM) of T1AM or resveratrol as an internal control using an ADP- or ATP-regenerating system for ATP synthase or ATPase activity respectively. To determine the minimal incubation times that permitted the establishment of equilibrium between the free enzyme and inhibitor with the enzyme-inhibitor complex, enzyme activity was measured as a function of time. These experiments showed that the steady-state condition was reached after 20 min, thus an incubation time of 25 min was applied in all experiments. Preliminary experiments run at the final concentrations achieved in the cuvette were carried out and showed that the equilibrium was maintained.

After incubation at pH 7.4, the activity assays were performed by addition of either 40μg SMP or ASp or 2 μg purified bovine F_1-ATPase to 1 mL of assay mixture at 37°C and following the changes in absorbance of NADPH or NADH at 340 nm. Initial rates (v) over a 60 s period were recorded. The ATP synthase assay mixture contained 10 mM HEPES pH 7.4, 20 mM succinate (i.e. the substrate of complex II in the respiratory chain that sustains the mitochondrial membrane potential $\Delta\psi$), 20 mM glucose, 3 mM $MgCl_2$, 4.78 units·mL^{-1} hexokinase, 2.2 units·mL^{-1} glucose-6-phosphate dehydrogenase, 10 mM KH_2PO_4, $NADP^+$ 0.75 mM, 11 mM AMP and 1 mM ADP (Cross and Kohlbrenner, 1978). The ATPase assay mixture contained 100 mM Tris/HCl pH 7.4, 50 mM KCl, 6 mM $MgCl_2$, 0.2 mM EDTA, 15 units·mL^{-1} pyruvate kinase, 15 units·mL^{-1} lactate dehydrogenase (Sigma), 0.23 mM NADH, 1 mM phosphoenolpyruvate and 4 mM MgATP (Zheng and Ramirez, 1999). When SMP and ASp were used, the ATPase assay mixture also contained rotenone (0.01 μg/μL), a complex I specific inhibitor, so that the enzyme could only hydrolyse ATP.

Oligomycin, a polyketide inhibitor of ATP synthesis and hydrolysis, which binds to the F_0 part of the complex, was used as a control in most of the kinetic analyses to determine the activity elicited by the assembled F_0F_1 complex, which represents around 90–95% of total activity in the mitochondrial particles.

IC_{50} is defined as the amount of T1AM required for 50% inhibition. Separate measurements made in the presence of MgADP showed that the inhibitors had no effect on the coupled assay systems.

Multiple inhibition kinetics for analysis of F_1-ATPase-T1AM interaction

To evaluate whether T1AM competition with a second inhibitor occurs on the F_1-ATPase, the Yonetani–Theorell plot was used (Yonetani and Theorell, 1964). Specifically, T1AM combinations with IF_1, resveratrol or aurovertin B were analysed. The semi-generalized formula shown below for a single enzyme multiple inhibition system by two reversible inhibitors was applied, where v_i and v_0 are the velocities of the inhibited and uninhibited reactions respectively (Martinez-Irujo *et al.*, 1998).

$$\frac{v_0}{v_1} = 1 + \frac{[I_1]}{K_{EI_1}\left(\frac{1+[S]/K_S}{1+[S]/\alpha K_S}\right)} + \frac{[I_2]}{K_{EI_2}\left(\frac{1+[S]/K_S}{1+[S]/\beta K_S}\right)} + \frac{[I_1][I_2]}{\gamma K_{EI_1} K_{EI_2}\left(\frac{1+[S]/K_S}{1+[S]/\alpha\beta K_S}\right)}$$

It follows that for situations where the binding of two inhibitors [I_1, I_2] to the enzyme is mutually exclusive, a plot of v_0/vi against [I_1] at a range of fixed [I_2] would give a series of parallel lines. On the other hand, if they can bind simultaneously to the enzyme, the slope will change with changing [I_2], and the series of lines will intersect.

IF_1 quantification by Western blot analysis in different SMP preparations and after treatment with inhibitors

Aliquots of IF_1-rich type I SMP were incubated with T1AM (up to 150 μM; 3.75 μmol·mg^{-1}), resveratrol (21 μM; 0.52 μmol·mg^{-1}) or aurovertin (0.1 μM; 2.5 nmol·mg^{-1}) for 15 min at 37°C and ATPase activity assayed. Reactions were stopped by ultracentrifugation, the supernatant completely removed and SMP suspended for immunoblot analysis.

For the quantification of IF_1 content (for methods, see Tomasetig *et al.*, 2002), ASp, type I and II SMP and type I SMP after treatment with inhibitors were separated by electrophoresis in a 15% SDS–polyacrylamide gel under reducing conditions. Proteins were transferred to nitrocellulose membranes, which were then incubated at room temperature for 1.5 h in 3% non-fat dry milk in PBS containing 0.1% Tween 20 (PBS–Tween). The membranes were incubated overnight at 4°C in PBS–Tween containing 3% non-fat dry milk with mouse anti-IF_1 (1:2000) or mouse anti-β (1:3000) (Mitosciences, Cambridge, UK). The membranes were washed three times in PBS–Tween and incubated in HRP-conjugated goat anti-mouse IgG (1:10 000). The membranes were rinsed in PBS–Tween, incubated with Pierce SuperSignal Dura chemiluminescence substrate and visualized with Image Scanner (Amersham). Signal intensities were quantified using ImageQuant TL program (GE Healthcare, Little Chalfont, Buckinghamshire, UK). Densitometric measurements were performed by Chemi doc XRS and analysed by Quantity One 4.2.1 Software (Biorad).

To determine the ratio between IF_1 and β subunits after treatment with different inhibitors, four quantities of each type I SMP sample (control and inhibitor treated) were simultaneously loaded into a gel and immunoblotted. A linear relationship was confirmed in each case between increasing band intensity and the quantities of proteins loaded into the gel, confirming non-saturating conditions. Quantitative data were inferred on the basis of the slope of the straight lines and reported as % of IF_1 against β subunit ratio with the control ratio taken as 100% (Contessi *et al.*, 2007). The results from four gels are expressed as means (±SD).

In situ *analysis of ADP-stimulated respiration in cardiomyocytes by high-resolution respirometry*

Rat cardiomyoblast-derived H9c2 cells (ATCC CRL1446), purchased from the American Type Culture Collection (Rockville, MD, USA) were grown as described by Comelli *et al.*, 2011. Oxygen consumption was measured by high-resolution respirometer Oxygraph 2k (Oroboros Instruments, Innsbruck, Austria) and expressed as pmol (10^6 s)$^{-1}$. H9c2 cells (1×10^6 cells·mL^{-1}) were re-suspended in respiration buffer (80 mM KCl, 10 mM Tris-HCl, 3 mM $MgCl_2$, 1 mM EDTA, 5 mM KH_2PO_4 pH 7.4) and permeabilized by digitonin (optimal concentration of 3.5 μg per 10^6 cells). After 10 min of incubation with T1AM at 37°C, saturating quantity of glutamate (10 mM), malate (5 mM) (resting respiration) and ADP (5 mM) (ADP-stimulated respiration) were added to the chamber. Cytochrome c (10 μM) was added in a parallel experiment to test for the intactness of the mitochondrial outer membrane in digitonin-treated cells. Data were digitally recorded using DatLab4 software (Oroboros); oxygen flux was calculated as the negative time derivative of oxygen concentration, cO2(t). Before performing the assays, air calibration and background correction were performed according to the manufacturer's protocol. The oxygen level was maintained above 40% air saturation.

Docking analysis

Docking of the ligand T1AM on F_1-ATPase was performed using the program Autodock Vina (Trott and Olson, 2010). The docking box was adjusted depending on the structure used for docking and had average dimensions of approximately 110 × 110 × 110 Å.

The starting receptor/target structures were taken from the Protein Data Bank corresponding to the apo form (i.e. ground state) of F_1-ATPase (pdb id. 1H8E, Abrahams *et al.*, 1994), F_1-ATPase bound to aurovertin B with ligand and all heteroatoms removed (pdb id. 1COW, van Raaij *et al.*, 1996), F_1-ATPase bound to resveratrol with ligand and all heteroatoms removed (pdb id. 2JIZ Gledhill *et al.*, 2007a) and F_1-ATPase bound to inhibitor IF_1 with ligand and all heteroatoms removed (pdb id. 2V7Q, Gledhill *et al.*, 2007b).

All forcefield parameters for T1AM (and for resveratrol and aurovertin B, for testing the docking procedure) were assigned using the program AutoDockTools (Morris *et al.*, 2009), starting with files in sdf format downloaded from the Pubchem database (URL: http://www.ncbi.nlm.nih.gov/). Rotatable bonds in the ligands were also assigned using the program AutoDockTools.

Two docking simulations were performed with aurovertin B and resveratrol in order to check whether the correctly bound form could be recovered from the best poses generated by simulation.

The exhaustiveness parameter, which controls the extent of conformational search in the program Vina, was raised to from 9 (default) to 50. The nine best poses were rotated such that they were placed in three approximately symmetrical positions in the ternary complex of αβ dimers. For the simulation with resveratrol, the centre of one of the poses was 0.2 Å distant from the centre of the original resveratrol binding, while for aurovertin B, one of the poses had a 0.5 Å centre-to-centre distance. The best poses were found for the original complex with the ligand removed.

For T1AM, the distance of the centre of mass of each pose from the centre of mass of aurovertin B and resveratrol was used as a criterion to identify common binding sites. On the contrary, due to the large extension of IF_1 in comparison with T1AM, the distance between the centres of mass is not significant. The maximum number of common atoms contacted by the ligands and IF_1 was considered instead.

Data analysis

Data are shown as means±SD, unless otherwise stated. Significant ($P < 0.05$) differences between group means were determined using the non-parametric two-tailed Student's t-test.

Materials

The phytochemicals, piceatannol and resveratrol (CalBiochem, Nottingham, UK), oligomycin and aurovertin B (Aldrich, Milwaukee, WI, USA), were prepared in ethanol as stock solutions (10 mM). T1AM was kindly provided by Dr T. S. Scanlan (Department of Physiology and Pharmacology, Oregon Health & Science University, Portland, OR, USA) and dissolved in 100% ethanol as a stock concentration (100 mM). All other chemicals and reagents were from Sigma Chemical Co. (St. Louis, MO, USA).

Results

The potency of T1AM in inhibiting the activity of purified soluble F_1-ATPase, which retains only reverse ATPase activity, was first evaluated and compared with that of resveratrol. Based on the IC_{50} values observed, the inhibitory potency of T1AM was similar to that of resveratrol (Figure 1A and B). The reversibility of T1AM inhibition was also demonstrated by precipitating F_1-ATPase and washing it in the absence of T1AM; samples that were inhibited up to 60% by T1AM subsequently recovered the same hydrolytic activity as control samples (data not shown).

Molecular docking analyses were then performed to predict the T1AM binding locations within the F_1-ATPase structure, whereby different target structures of the protein were analysed. Docking simulations with T1AM were first performed using the crystallographic structures of the enzyme inhibited by two well-characterized inhibitors (the antibiotic aurovertin B and the natural inhibitor protein IF_1) in addition to the phytochemical resveratrol. Binding regions are shown in Figure 2B–D. The crystallographic structures of aurovertin B-inhibited (pdb id. 1COW), resveratrol-inhibited (pdb id. 2JIZ) and IF_1-inhibited (pdb id. 2V7Q) F_1-ATPase were considered following removal of the inhibitor. This approach

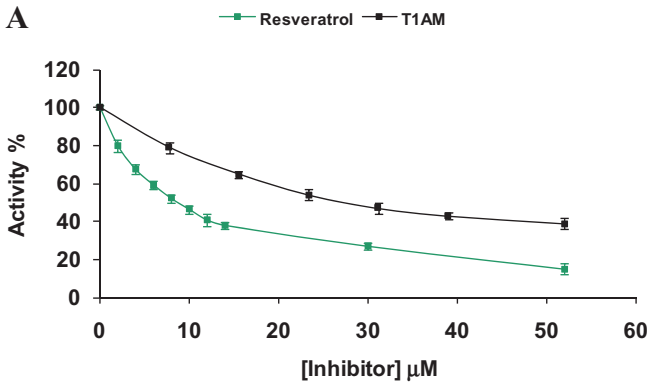

B

	IC_{50}
T1AM	**27.5 ± 1.4 μM** *13.75 μmol (mg F_1)$^{-1}$; n=4*
Resveratrol	**8.7 ± 0.8 μM** *4.35 μmol (mg F_1)$^{-1}$; n=5*

Figure 1

Effect of T1AM and resveratrol on F_1-ATPase activity. F_1-ATPase was incubated with T1AM (7.8–52 μM) or resveratrol (2–52 μM), and ATPase activity was assayed. In panel A, results are expressed as percentage residual activity and are means (± SD) of four and five independent experiments for T1AM and resveratrol, respectively. Control F_1-ATPase activity was 87.4 ± 2.4 μmol ATP hydrolysed min^{-1}(mg protein)$^{-1}$ and was set as 100%. In panel B, the IC_{50} values for both inhibitors are shown. The values are expressed as both μM and μmol (mg F_1-ATPase)$^{-1}$.

enabled us to assess whether T1AM could fit into known binding cavities. Docking simulations, starting from the F_1-ATPase ground state (pdb id. 1H8E), were performed in order to confirm whether binding occurred to the known inhibitory regions and provide clues with regard to other possible binding sites. The rigid structure of the target most likely results in non-optimal binding because conformation rearrangements are not allowed.

The shortest distances between the centre of mass of aurovertin B, resveratrol and T1AM and the centre of mass of each of the two inhibitors, resveratrol and aurovertin B, found in a pose for all the different F_1-ATPase target conformations, are reported in Table 1. It should be noted that these distances depend on the starting target conformation. For both aurovertin B and resveratrol, poses with the same overlap in the known binding sites were found for the inhibited-enzyme complexes with the respective inhibitors removed. Confident results were obtained only after raising the exhaustiveness of the docking search in Vina (see Methods). With the same target structures, poses for T1AM were found within both aurovertin B and resveratrol binding sites (Figure 2B and C respectively). In poses in which the ground state structure was a target, the centre of mass distances between the known inhibitor sites and each of the inhibitors were greater. The maximum number of F_1-ATPase common atoms contacted by each chemical inhibitor and IF_1

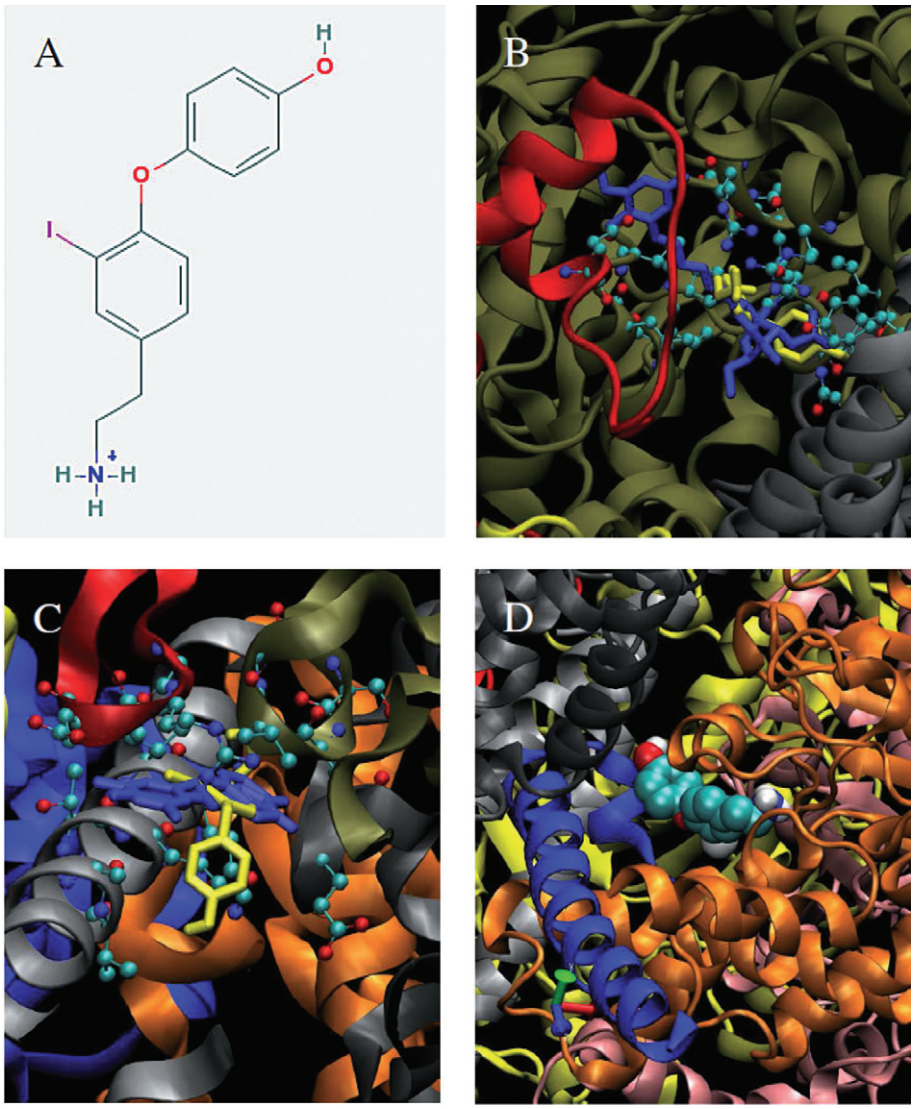

Figure 2

Molecular docking of T1AM into aurovertin B, resveratrol and IF_1 binding sites of F_1-ATPase. The chemical structure of T1AM consisting of one phenolic ring and one 3-iodophenylethylamine ring is shown in panel A, Three hypothetical T1AM binding locations within the F_1-ATPase structure obtained by the docking analysis approach (Autodock Vina) are shown in panels B, C and D. In panel B, the aurovertin B binding region is shown; F_1 is shown as a red (B chain, α subunit) and green (F chain, β subunit) cartoon, aurovertin is in blue, the T1AM molecule is in yellow, and F_1 residues contacting aurovertin and/or T1AM are in ball and stick format (coloured by atom type). In panel C, the resveratrol binding region of F_1 and the partial overlapping of T1AM is shown; F_1 is in cartoon coloured by chain, resveratrol is in blue and the T1AM molecule in yellow. In panel D, the overlap between the IF_1 binding site and the T1AM binding region is shown; T1AM is shown as van der Waals spheres (coloured by atom name) together with IF_1 (dark blue cartoon) and F_1 (cartoon coloured by chain).

found in a pose for all the different target structures is also reported in Table 1. Overlap with the IF_1 binding site was found in poses that started from all target conformations, except for the IF_1-inhibited complex, suggesting that this region could be bound by T1AM with no conformational rearrangements.

To emphasize the overlap between the T1AM and IF_1 binding locations, T1AM is shown as van der Waals spheres in Figure 2D, together with IF_1 (dark blue cartoon) and F_1 (cartoon coloured by chain). The poses closer to the aurovertin binding site were also those with the largest overlap with the IF_1 binding site.

The inhibitory effect exerted by T1AM was further analysed on the F_0F_1-ATP synthase whole enzyme complex in mitochondrial membranes. First, the effect of T1AM on ATPase-synthase activity was assayed on type II SMP obtained in the presence of succinate using a standard protocol (Ferguson *et al.*, 1977). Considering the T1AM inhibitory effect on respiratory chain observed in rat liver (Venditti *et al.*, 2011), in order to minimize ATP synthesis inhibition not due to direct interaction with the enzyme, T1AM inhibitory potency upon ATP synthase activity was evaluated supplying succinate to sustain $\Delta\psi$. In muscle, in contrast to liver mitochondria, the complex II substrate is known to sustain respi-

Table 1

Autodock Vina docking analysis data

Target	Distance from aurovertin site			Distance from resveratrol site			Overlap with IF_1 site		
	Aur	Resv	T1AM	Aur	Resv	T1AM	Aur	Resv	T1AM
F_1 ground state	13.9 Å	15.7 Å	**5 Å**	5.6 Å	2.3 Å	**11.8 Å**	20	0	**9**
F_1-IF_1	14.6 Å	14.5 Å	**17.8 Å**	6.1 Å	8.6 Å	**12.3 Å**	5	5	**0**
F_1-resv	14.0 Å	15.6 Å	**11.5 Å**	5.9 Å	0.2 Å	**1.1 Å**	0	0	**10**
F_1-aur	0.5 Å	31.3 Å	**4.9 Å**	6.2 Å	1.4 Å	**1.0 Å**	10	0	**7**

Rows indicate the target structure used for docking. In the first three columns, the shortest distance (among the best nine poses) between each ligand's centre of mass, that is aurovertin (aur), resveratrol (resv), T1AM (T1AM) and the centre of mass of aurovertin in complex with F_1, are shown. In the next three columns, the same distances are reported from the centre of mass of resveratrol in complex with F_1. In the last three columns, the maximum number of atoms contacting the three ligands (among the best nine poses) at the IF_1/F_1 interface is shown.

ration with lower efficiency than those of complex I (see Gnaiger, 2009). We confirmed in separate control experiments on permeabilized heart-derived cells, this difference in efficiency: the values of ADP-stimulated respiration were 131 ± 21.8 pmol $(10^6\ s)^{-1}$ for complex I and 45.1 ± 19.5 pmol $(10^6\ s)^{-1}$ for complex II. Thus, in the presence of succinate, T1AM was able to produce minor effects on respiratory complexes (Venditti *et al.*, 2011). The IC_{50} values (28.2 ± 2.4 μM) indicate that the inhibitory potency of T1AM upon ATP synthase activity is similar to that of resveratrol (29.9 ± 1.7 μM) (Figure 3A and B). Conversely, when Δψ was reduced by rotenone, T1AM exerted a very low inhibitory effect upon ATPase activity (starting at 50 μM inhibitor) that did not allow us to calculate the IC_{50} value (Figure 3A). The IC_{50} of resveratrol in type II SMP upon ATPase activity (monitored as a control) was 20.1 ± 0.4 μM (Figure 3B), similar to its potency upon ATP synthase activity (29.9 ± 1.7 μM), in accordance with Zheng and Ramirez, (2000). This apparent discrepancy may be due in part to some inhibitory effect that T1AM may elicit on the electron transport system.

Nevertheless, we also hypothesized that IF_1 bound to the enzyme could affect the inhibitory action of T1AM but not of resveratrol on ATPase activity, in line with the overlap between the T1AM and IF_1 binding locations observed by molecular docking. To test this hypothesis, the inhibitory potency of T1AM was evaluated on F_1-ATPase upon treatment with IF_1 concentrations in the range of the IC_{50}. As shown in Figure 4, activation of IF_1-inhibited F_1-ATPase occurs after treatment with T1AM starting from 50 nM, and is more evident at higher IF_1 concentration (50% inhibition), proving that T1AM binds with high affinity to F_1-ATPase and favours IF_1 displacement. Interestingly, a statistically significant inhibitory effect by T1AM *per se* starts to be recorded only at 350 nM. The inhibitory potency of T1AM, compared with resveratrol, against ATPase activity was also evaluated in particles with different IF_1 contents, i.e. IF_1-rich type I SMP and IF_1-stripped ASp. IF_1 quantities were determined by immunoblot analysis, showing that type I SMP contained an IF_1 quantity approximately double that of type II SMP, while ASp contained negligible amounts of IF_1 (Figure S1). The effect of T1AM was analysed over a large range of concentrations. As observed for soluble F_1-ATPase, activation of the whole enzyme is elicited in type I SMP in the low nanomolar range

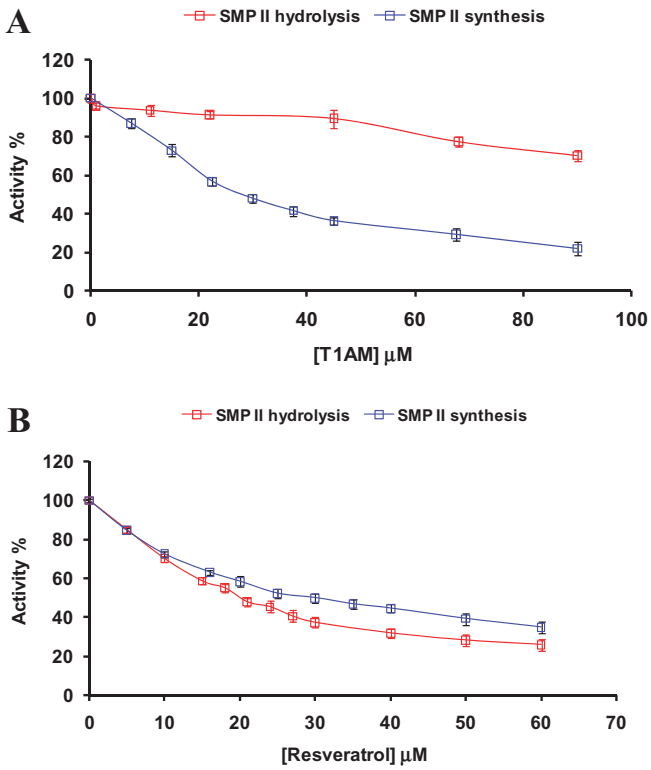

Figure 3

Effect of T1AM and resveratrol on the F_0F_1-ATPase/synthase activity in type II SMP. Type II SMP were incubated at pH 7.4 with T1AM (1–90 μM) or with resveratrol (5–60 μM), and ATPase or ATP synthase activity was assayed as described in the Methods section. In panel A, ATPase and ATP synthase activities after treatment with T1AM are shown expressed as percentage residual activity. In panel B, ATPase and ATP synthase activities after treatment with resveratrol are shown expressed as percentage residual activity. Data are expressed as means (± SD) of at least three independent experiments.

of T1AM (Figure 5, inset panel A). A significant activation was not observed on type II SMP probably as consequence of the lower amount of IF_1 bound in the enzyme, together with limits in sensitivity of the spectrophotometric assay. On the

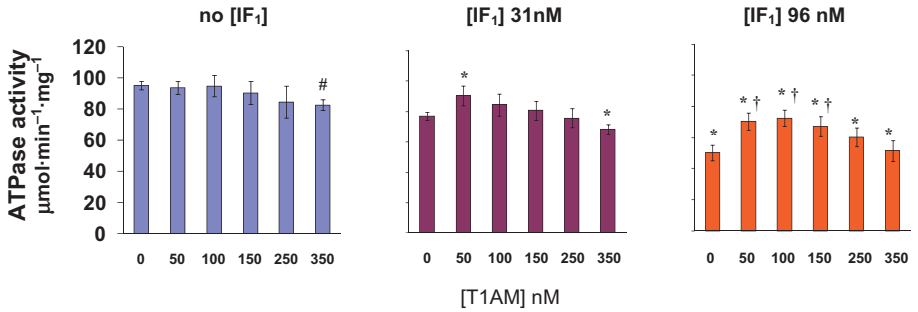

Figure 4

Effect of T1AM on IF_1-inhibited F_1-ATPase. Soluble F_1-ATPase (5.2 nM) was preincubated in the absence or in the presence of IF_1 (31 or 96 nM), and effects of T1AM (50–350 nM) on ATPase activity were assayed. Results are expressed as residual activity and are means (± SD) of three independent experiments. Control F_1-ATPase activity was 95.2 ± 2.7 µmol ATP hydrolysed min^{-1}(mg protein)$^{-1}$. Statistic significance of the differences was calculated with Student's *t*-test for independent groups: *: $P < 0.005$ significantly different from T1AM-treated/IF_1-untreated correspondent samples. #: $P < 0.05$ significantly different from T1AM-untreated/IF_1-untreated controls. †: $P < 0.005$ significantly different from 31 or 96 nM IF_1-treated/T1AM-untreated correspondent samples.

contrary, an inhibitory effect was observed with type II SMP after treatment with micromolar T1AM, although the IC_{50} value could not be calculated from this slight inhibition (Figure 5A). The IC_{50} value of T1AM against whole enzyme in membrane was calculated in IF_1-stripped ASp to be 73.7 ± 4 µM (Figure 5C). These data confirm our hypothesis that the presence of IF_1 bound in F_0F_1-ATP synthase influences the effect of T1AM, suggesting a competition between IF_1 and T1AM for binding to F_0F_1. This does not occur in the case of resveratrol, as expected on the basis of the similar IC_{50} values for ATPase and ATP synthase activity in type II SMP and the low frequency of common contacts with IF1 in the docking analyses. In fact, the IC_{50} values in type II SMP, type I SMP and ASp were 20 ± 0.8, 19.1 ± 1.5 and 21.2 ± 1.2 µM respectively (Figure 5C). In summary, the dual effect exerted by T1AM may be consistent with the presence of distinct binding locations, as suggested by docking analysis, with different affinities.

To further confirm our hypothesis that T1AM binding leads to the displacement of IF_1, IF_1 content was quantified by immunoblotting in IF_1-rich type I SMP after treatment with T1AM (at 0.4–150 µM). Both resveratrol and aurovertin B were used as controls (Figure 6A and B). This approach allowed us to monitor a progressive decrease in residual IF_1 quantities (i.e. an increase in IF_1 release) as T1AM concentrations increased (Figure 6C), showing an asymptotic trend. IF_1 release occurring in this assay even at micromolar T1AM concentration is likely to be due to the experimental procedure, that is SMP sedimentation and supernatant removal. Conversely, treatment with aurovertin B or resveratrol at concentrations close to the IC_{50} values only slightly reduced (around 30%) or had no effect upon IF_1 content (Figure 6B), indicating that the experimental procedure affects the binding equilibrium provided that the binding is destabilized. Together, these data confirm that IF_1 is displaced by T1AM via its high-affinity binding to the enzyme, in accordance with a possible binding location for T1AM lying within the IF_1 binding region as observed by molecular docking.

Of note, the inhibitory potency of T1AM against F_1-ATPase is close to that of resveratrol (Figure 1A and B) and similar to that observed in ASp (Figure 5C), and no inhibition was registered after incubation with low concentrations of T1AM up to 0.25 µM (Figure 4), in accordance with the absence of IF_1 in F_1-ATPase preparations. Thus, the F_1-ATPase model was used to characterize the inhibition exhibited by T1AM at micromolar concentrations and to explore the localization of the T1AM inhibitory region/site by multiple inhibitor competition analysis.

As shown by Lineweaver–Burk plots of F_1-ATPase activity at different ATP concentrations (0.125–4 mM), T1AM exerted non-competitive inhibition (Figure S2A), whereas control experiments confirmed a mixed type inhibition for resveratrol (Figure S2B). The Km at different concentrations of T1AM, calculated as the intercept of each plot with the *x* -axis, was found to be unchanging: 0.69 ± 0.03 mM. The apparent Vmax was 152.5 ± 2.1 µmol of ATP hydrolysed min^{-1} mg^{-1} in the absence of T1AM and reduced to 96.1 ± 2.8 and 64.9 ± 2.4 µmol ATP in the presence of 18 and 35 µM of T1AM respectively. The K_i, an index of the inhibitory potency of T1AM, was calculated using the v_i/v_0 ratio over the concentration range of T1AM (7.8–52 µM) and found to be 29.8 ± 3.0 µM which is compatible with the IC_{50} value (Figure 1B).

Furthermore, competition experiments using T1AM with multiple inhibitors were performed as reported in Gledhill and Walker (2005). The combination of T1AM with IF_1, resveratrol or aurovertin B was analysed by means of the Yonetani–Theorell plot (Yonetani and Theorell, 1964) to determine whether T1AM competes with these inhibitors in a mutually exclusive manner. A competition experiment using resveratrol and piceatannol, performed as a control, confirmed the data obtained by Gledhill and Walker (2005), which indicated that the two polyphenolic phytochemical inhibitors bind to the same site (data not shown). The competition of T1AM and IF_1 was analysed for different concentration ranges based on the respective inhibitory potency, that is 15–45 nM for IF_1 and 5–20 µM for T1AM. The plots of v_0/v_i against IF_1 (I_1) at various concentrations of T1AM (I_2) and *vice versa* generated a series of parallel straight lines (Figure 7A and B). These results indicate the mutually exclusive binding of IF_1 and T1AM to F_1-ATPase, most likely as a consequence of

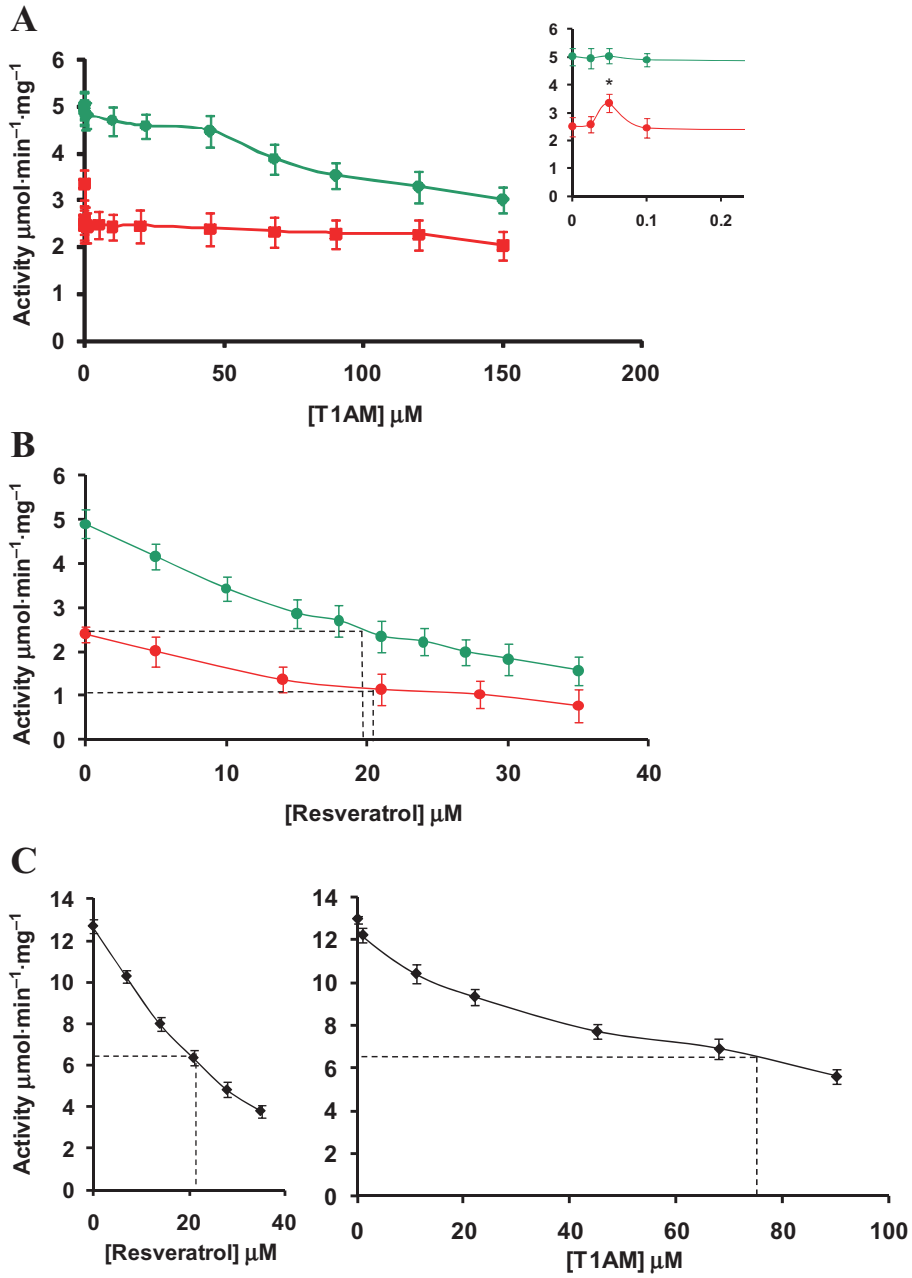

Figure 5

Effect of T1AM and resveratrol on F_0F_1-ATPase activity in type I SMP, type II SMP and ASp containing different amounts of IF_1. Type I SMP, type II SMP and ASp were incubated with T1AM or resveratrol, and ATPase activity was assayed. Panel A shows the plot of the ATPase activity (as µmol·min^{-1}·mg^{-1}) of SMP I and SMP II against 0.025–150 µM T1AM concentration (n = 4). In the inset, the range between 0.025 and 0.2 µM T1AM is enlarged; * P< 0.05, significant activation of ATPase. Panel B shows the plot of the ATPase activity of SMP I and SMP II against 0.05–35 µM resveratrol concentration (n = 4). The plots in panel C report ATPase activity of ASp against resveratrol (0.5–35µM) and T1AM (0.025–90 µM) (n = 3). Dotted lines indicate the IC_{50} values of resveratrol on SMP I and SMP II (panel B) and of both resveratrol and T1AM on ASp (panel C). Control F_0F_1-ATPase activity was 2.5 ± 0.3 µmol ATP hydrolysed min^{-1}(mg protein)$^{-1}$ (n = 3) for type I SMP, 4.9 ± 0.3 µmol ATP hydrolysed min^{-1}(mg protein)$^{-1}$ (n = 3) for type II SMP, and 13.0 ± 0.4 µmol ATP hydrolysed min^{-1}(mg protein)$^{-1}$ (n = 3) for ASp. Data shown are means ± SD.

partially overlapping binding sites or the distortion of reciprocal sites induced by T1AM-F_1-ATPase or IF_1-F_1-ATPase complex formation. Competition data are in accordance with IF_1 displacement and with a possible binding location for T1AM lying within the IF_1 binding region as observed by molecular docking analyses. The inhibitory effect that IF_1 was still able to achieve despite micromolar concentrations of T1AM (Figure 7A and B) could be explained by the hypothesis that T1AM binding to the low affinity region/site reduces the negative control exerted by the high-affinity region/site on

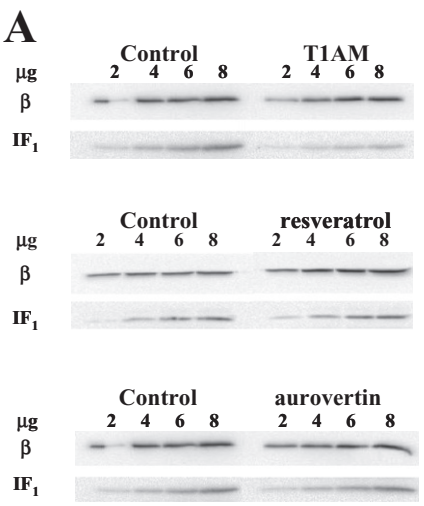

B

	%
Control	**100**
T1AM *3.75 μmol (mg protein)$^{-1}$ (150 μM)*	**24.6 ± 3.7**
T1AM *0.52 μmol (mg protein)$^{-1}$ (21 μM)*	**57.2 ± 3.4**
Resveratrol *0.52 μmol (mg protein)$^{-1}$ (21 μM)*	**96.5 ± 4.5**
Aurovertin B *2.5 μmol (mg protein)$^{-1}$ (0.1 μM)*	**72.2 ± 4.7**

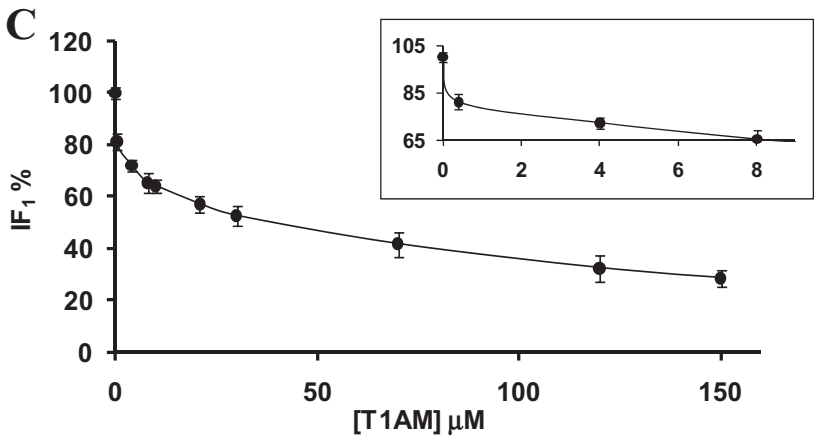

Figure 6

Quantification of IF_1 in IF_1-rich Type I SMP after treatment with inhibitors. Type I SMP were pre-incubated in the absence or presence of different concentrations of T1AM, resveratrol or aurovertin. IF_1 displaced from F_0F_1-ATP synthase was removed by ultra centrifugation of the supernatant and the SMP sediment resuspended in medium without inhibitors. Panel A shows a representative image of the immunoreactive bands relative to different quantities of protein separated by SDS-PAGE, transblotted and identified with specific antibodies against the F_0F_1-ATP synthase β subunit and IF_1. The concentrations of the inhibitors in the experiment shown were as in panel B, except for T1AM which was used at 150 μM. In panel B, quantitative data inferred by densitometric analysis of immunoreactive bands are summarized. Values are expressed as percentages. IF_1 was normalized to F_0F_1-ATP synthase β subunit (β) quantities, as described in the Methods section, with the IF_1/β ratio of untreated control samples considered as 100%. Values are means (± SD) of at least three independent experiments. Panel C shows the plot of IF_1/β (%) against T1AM concentration (0.4–150 μM). The inset shows an enlargement of the change in IF_1 amounts at the lowest T1AM concentrations.

IF_1 binding, as also suggested by the data shown in Figures 4 and 5.

The Yonetani–Theorell plot obtained for T1AM and aurovertin B gave a series of parallel lines (Figure 7C), again indicating the mutually exclusive binding of T1AM to F_1-ATPase, in line with overlapping of the T1AM and aurovertin B binding locations as revealed by molecular docking analyses. Intersecting lines were observed in a similar plot for T1AM with resveratrol (Figure 7D), indicating that the two compounds bind to different sites, contrary to what suggested by the modelling data.

Finally, to further corroborate the activating effect elicited by T1AM on F_0F_1-ATP synthase, we investigated if such an effect was observed on mitochondrial ATP synthesis under more physiological conditions, i.e. in whole cells. *In situ* respirometric analysis was performed on H9c2 cardiomyocytes at low nanomolar concentrations of T1AM. An increase in ADP-stimulated mitochondrial respiration with no effect on resting respiration was observed, indicating an activation of F_0F_1-ATP synthase. A representative experiment carried out at 50 nM T1AM is shown in Figure 8. In order to estimate the molar ratio between endogenous IF_1 and the putative competitor T1AM added to permeabilized cells, we quantified IF_1 content by quantitative immunoblotting on H9c2 total homogenates, using a calibration plot with purified IF_1 as a standard (Figure S3). The value of IF_1 content obtained was 2.04 ± 0.36 pmol mg^{-1}, that is equivalent to about 2 μM. This is considerably in excess of the concentration iof T1AM

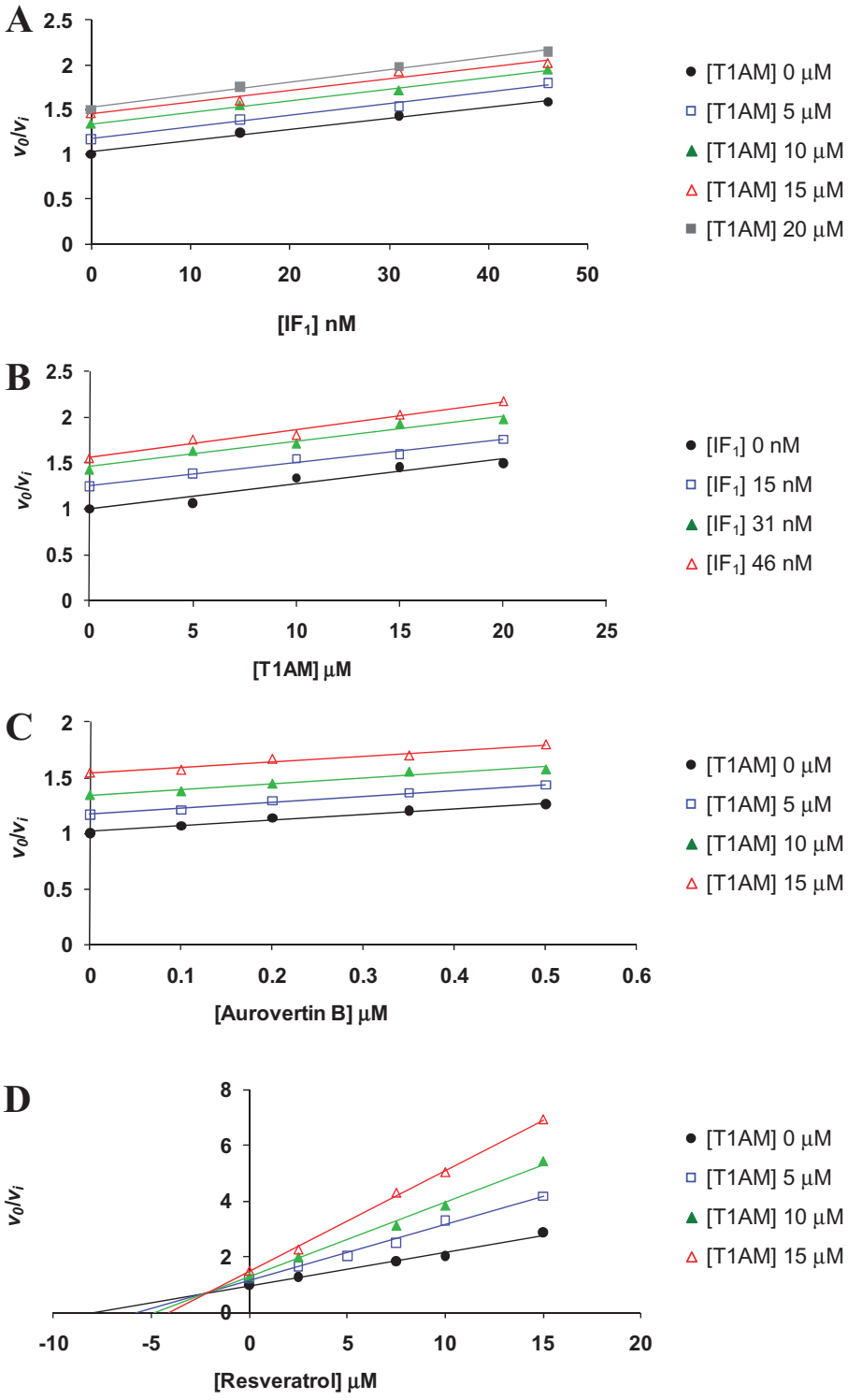

Figure 7

Multiple inhibitor analysis on F_1-ATPase: Yonetani–Theorell plots for the combination of T1AM with IF_1, aurovertin B or resveratrol. Plots of F_1-ATPase v_0/v_i against $[I_1]$ at a range of fixed $[I_2]$ are reported. The panels show the combination of micromolar T1AM with IF_1 (A and B), aurovertin B (C) and resveratrol (D). Linear regression lines are drawn through the data points ($0.996 < R^2 < 0.999$) in each plot. Each data point is independent of all others. The use of at least 20 points is sufficient to determine the nature of the interaction between multiple inhibitors (Gledhill and Walker, 2005).

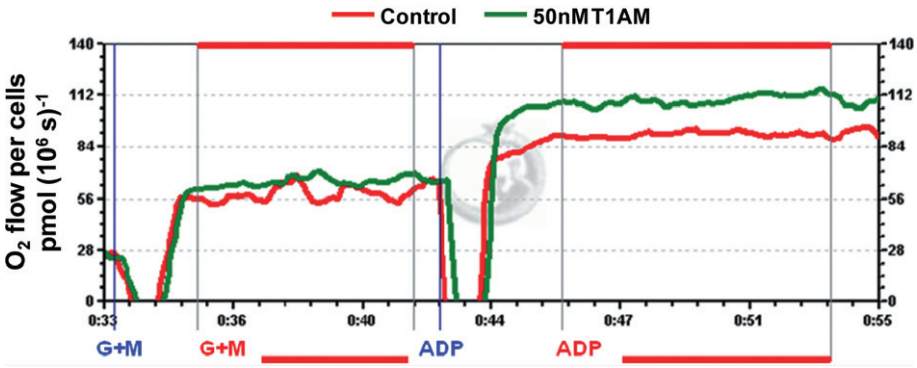

Figure 8

Effect of T1AM upon ADP-stimulated mitochondrial respiration of digitonin-permeabilized H9c2 cells. Representative oxygen flow records (high-resolution respirometer Oxygraph 2k) are reported for cells pre-incubated with 50 nM T1AM and control samples. Respiratory rates sustained by complex I were measured in two metabolic states – resting respiration and ADP-stimulated respiration. Metabolic substrates (G, glutamate, M, malate; and ADP; in blue) were added to the chamber at concentration specified in Methods. Analysis sections (in red) were marked when signal stability was reached. One experiment representative of three (SD < 18%).

added (50nM) so our results showing activation of mitochondrial ATP synthesis suggest that the mitochondria may have concentrated T1AM. At about 6 μM, T1AM should be able to compete with IF_1, on the basis of threefold excess of competitor required *in vitro*, as indicated by Figures 4 and 5. Thus, our data indicate that T1AM can be concentrated inside H9c2 mitochondria without reaching, under the experimental conditions used, an ATP synthase-inhibiting concentration (see data reported in figure 3A).

Discussion

F_0F_1-ATP synthase plays a critical role in both human health and disease and it represents a promising therapeutic target for the treatment of diseases, such as cancer, diabetes, heart disease, mitochondrial myopathies, neurodegenerative diseases and immune disorders (see Hong and Pedersen, 2008; Lippe *et al.*, 2009; Johnson and Ogbi, 2011). Thus, a better understanding of F_0F_1-ATP synthase inhibition and regulation may aid the treatment of these diseases.

T1AM is a novel endogenous chemical messenger formed during thyroxine metabolism (Scanlan *et al.*, 2004), which has been found *in vivo* in several tissues of mouse and rat, as well as in human blood (Galli *et al.* 2012). Its intracellular concentration exceeds that of tri-iodothyronine (T_3) by about 10-fold in most tissues, including the heart (Saba *et al.*, 2010). Non-genomic effects of thyroid hormone-related compounds have been known for a long time; nevertheless, the molecules and mechanisms that trigger such effects have not been completely elucidated. There is already evidence that T1AM may mediate such effects (Ianculescu and Scanlan, 2010; Frascarelli *et al.*, 2011) and T1AM deserves particular attention as it does not interact with thyroid hormone receptors, but rather with membrane GPCRs and possibly with intracellular binding sites (Scanlan *et al.*, 2004; Piehl *et al.*, 2011).

The effects of thyroid hormone and its derivatives on mitochondrial energy production, as well as the finding that intracellular transport (Ianculescu *et al.*, 2009) gives T1AM access to mitochondrial targets (Frascarelli *et al.*, 2011), prompted us to investigate T1AM interaction with F_0F_1-ATP synthase *in vitro*. As T1AM was shown here to interact with F_0F_1-ATP synthase, by exerting a dual effect upon the enzyme activity, the range of endogenous compounds known to bind to and regulate F_0F_1-ATP synthase is extended.

Because of the physiological and pathological roles exerted by IF_1 in F_0F_1-ATP synthase regulation (Rouslin *et al.*, 1995; Green and Grover, 2000; Contessi *et al.*, 2004; Penna *et al.*, 2004; Comelli *et al.*, 2007), the IF_1-displacing effect of T1AM is an intriguing result and is reinforced by the data from the molecular docking analyses, which suggest that T1AM may bind within the IF_1 binding cavity, related by approximate symmetry to the aurovertin binding site. The overlap of T1AM docking with the IF_1 binding site was found in poses arising from all the target starting conformations of the enzyme except the IF_1-inhibited (i.e. resveratrol-inhibited, aurovertin B-inhibited and ground state F_1-ATPase), suggesting that the binding of T1AM within the IF_1 binding region likely occurs with negligible conformational rearrangements. The biochemical approaches allowed us to demonstrate that the binding of T1AM to F_0F_1-ATP synthase did actually occur and was mutually exclusive with the binding of IF_1. These conclusions were based on the following findings: (i) the effects of T1AM on the ATPase activity observed with IF_1-inhibited F_1ATPase and different IF_1-containing particles; (ii) the results of immunodetection of the residual IF_1 content of the particles upon exposure to T1AM; and (iii) the results of T1AM–IF_1 competition analyses. From these results, we can confidently state that when T1AM binds to the F_1 sector at low nanomolar concentrations, it favours the release of IF_1 from its binding site, which is located on a catalytic interface between the C-terminal regions of the α_{DP}- and β_{DP}- subunits. Hence, we named the T1AM high affinity-binding site as 'IF_1-displacing high-affinity site'.

Based on the IF_1-displacing effect shared by T1AM and the antibiotic aurovertin B (Johnson *et al.*, 2009), we performed docking analyses and compared their inhibitory effects.

Aurovertin B is known to bind to F_1-ATPase and to occupy a cavity situated on the cleft between the nucleotide-binding and C-terminal domains of the β-subunits, as depicted by crystallographic data (van Raaij *et al.*, 1996). Docking analyses for the T1AM molecule performed in the aurovertin B binding cavity of all the above mentioned F_1-ATPase inhibited structures depleted of inhibitor, as well as in the ground state structure, suggested that a T1AM binding site could be located within the aurovertin B binding cavity. Kinetic experiments revealed that (i) T1AM bound with a low affinity, thereby eliciting inhibitory effects (micromolar range); and (ii) its binding appeared to be mutually exclusive with that of aurovertin B. Thus, T1AM may bind within the aurovertin B binding site. In line with results observed at micromolar concentration on type II SMP, the inhibitory effects of T1AM on ATPase activity may well be counteracted by T1AM binding to the 'IF_1-displacing high-affinity site'. Indeed, IF_1 release caused an increase in the amount of active ATPase molecules, thereby making ligand concentration limiting. Accordingly, no inhibitory effect was observed with IF_1-rich type I SMP, where at low T1AM concentrations, an activating effect indicative of IF_1 release was observed and the two effects are apparently balanced. Hence, we postulated a second T1AM binding site and we named it as 'aurovertin-displacing low affinity-site'.

Of note, T1AM appears to be a significantly more potent inhibitor of ATP synthesis than ATP hydrolysis. This may be partially a consequence of T1AM inhibition of complex III of the respiratory chain, which as been recently reported (Venditti *et al.*, 2011). Nevertheless, as similar differential effects were reported for aurovertin (Lenaz, 1965; Lee and Ernster, 1968; Roberton *et al.*, 1968; Bertina *et al.*, 1973), an alternative explanation may be that previously suggested for aurovertin (Johnson *et al.*, 2009). These authors showed that aurovertin elicited a paradoxical activating effect of ATP hydrolysis at low concentrations of substrate, which was connected to dissociation of IF_1 from the F_1 domain. This hypothesis was confirmed in the present study by immunoblotting analysis documenting a significant release of IF_1 from F_0F_1-ATP synthase, following treatment of IF_1-rich type I SMP with aurovertin. Notably, this effect was smaller than that observed with T1AM and in accordance with the finding that aurovertin exerted similar inhibitory effects on IF_1-free F_1-ATPase and IF_1-containing SMP particles (Hong and Pedersen, 2008).

In line with the IF_1-displacing effect shared by T1AM and aurovertin B and the proximity of the aurovertin B and IF_1 sites defined by crystallography (van Raaij *et al.*, 1996; Cabezon *et al.*, 2003), we suggest a reciprocal influence between the T1AM binding sites. Thus, the activation exerted by T1AM on IF_1-inhibited F_1-ATPase and IF_1-rich type I SMP at low nanomolar but not at higher concentrations can be explained by the hypothesis that T1AM binding to the low affinity region/site reduces the negative control exerted by the high-affinity region/site on IF_1 binding. Such a mutual interaction between the two sites also justifies the mutual exclusive binding of IF_1 and T1AM at micromolar concentrations.

Many polyphenols have been shown to bind to and inhibit F_0F_1-ATP synthase, and the potentially relevant effects of natural dietary polyphenolic compounds as antimicrobial and anti-tumour agents are proposed to be partly linked to the inhibition of ATP synthesis (Pirola and Frojdo, 2008). The polyphenol binding pocket is well known and is located between the tip in the C-terminal region of the γ subunit and the β_{TP} subunit (Gledhill *et al.*, 2007a). Although our modelling analysis, performed by docking the T1AM molecule into the three F_1-ATPase inhibited structures, also suggests the resveratrol site as a putative location for T1AM, the competition experiments indicated that resveratrol and T1AM binding are not mutually exclusive. Thus, the possibility that T1AM may bind to the resveratrol site can be excluded.

Representation of T1AM binding regions in F_0F_1-ATP synthase structure

The binding regions of the three known inhibitors in the F_1-ATPase structure are depicted in Figure 9; three putative T1AM locations are denoted by circles. These binding regions may be consistent with the particular dual effect elicited by T1AM, as demonstrated by our data, as well as with mutual influence between the sites. As mentioned above, docking analyses suggest that the aurovertin B site is a possible binding site for T1AM. Poses were found in the experimental cavities revealed by X-ray crystallography and also in a region overlapping the IF_1 binding site, which is approximately symmetry-related to the two aurovertin binding sites. Thus, considering the proximity of the aurovertin B and IF_1 sites defined by crystallography (van Raaij *et al.*, 1996; Cabezon *et al.*, 2003), we suggest that the T1AM 'IF_1-displacing high-affinity site' could be either the site overlapping with IF_1 related by approximate symmetry with aurovertin binding sites, or one of the two aurovertin binding sites, even as one of these could be T1AM 'aurovertin-displacing low affinity-site'. A reciprocal influence between the T1AM putative binding sites is suggested by the similarity of behaviour of T1AM and aurovertin.

Nevertheless, the higher IF_1-displacing efficiency of T1AM with respect to aurovertin B, together with T1AM proximity (docking analysis) to IF_1 residues 1–7, which are reported to contribute to the destabilization of the binding of IF_1 to F_1 (Bason *et al.*, 2011), allows us to hypothesize that the T1AM 'IF_1-displacing high-affinity site' most likely overlaps with the IF_1 binding site.

Considerations on physiopathological or pharmacological impact

T1AM is an endogenous compound that has been detected in many different tissues. In rat, the highest T1AM levels were observed in liver, brain and kidney, where overall T1AM concentration ranged from 36 to 93 pmol g^{-1} (i.e. around 40–90 nM) (Saba *et al.*, 2010). The effects elicited on intact mitochondria indicated that it can enter mitochondria (Venditti *et al.*, 2011). On the basis of our findings, we suggest that the effect of T1AM binding, impairing IF_1 inhibitory efficiency, could be of physiological or pathological relevance, and that endogenous T1AM may represent another endogenous factor (in addition to pH, $\Delta\mu H^+$ and ATP, Ca^{2+} and Mg^{2+} levels) involved in the modulation of the steady-state binding of IF_1 to F_0F_1-ATP synthase. Such effects may be particular relevant in the heart, where recent experiments have shown that T1AM reaches a concentration (6.6 pmol g^{-1}, i.e. around

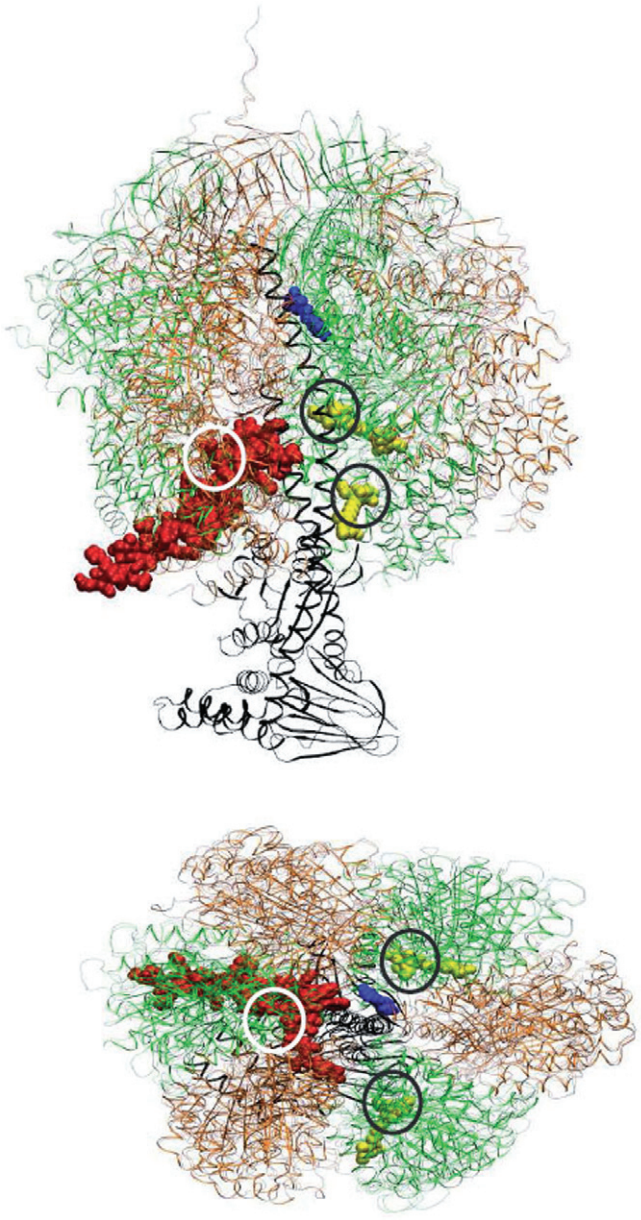

Figure 9

Putative T1AM binding regions that overlap with the IF_1, aurovertin B but not resveratrol binding sites in F_1-ATPase. The side view of the F_1-ATPase structure and the view along the central axis from the catalytic sites towards the membrane are shown. IF_1 (red, van der Waals spheres), aurovertin B (yellow, van der Waals spheres) and resveratrol (blue, van der Waals spheres) inside their respective binding sites are shown (structures from Protein Data Bank). T1AM binding regions predicted using the Autodock Vina program (Trott and Olson, 2010) and confirmed by kinetic data are indicated by circles (white circle indicate the site overlapping with IF_1 binding site; black circles indicate the sites overlapping with aurovertin binding sites). Images were produced using the program Visual Molecular Dynamics (Morris *et al.*, 2009). Based on the model depicted, the so-called IF_1-displacing high-affinity site of T1AM could be either the site overlapping with IF_1 related by approximate symmetry with aurovertin binding sites, or one of the two aurovertin binding sites, which could correspond to the so-called aurovertin-displacing low affinity-site.

10 nM) 20-fold higher than that in the extracellular compartment both *in vivo* and *ex vivo*. Accordingly, isolated cardiomyocytes are able to take up exogenous T1AM, establishing a 30-fold gradient between intracellular and extracellular concentration (Saba *et al.*, 2010).

In whole cells, using *in situ* respirometric analysis on H9c2 cardiomyocytes treated with T1AM at a concentration in the order of 50 nM, we observed an increase of ADP-stimulated respiration, indicating an activation of mitochondrial ATP synthesis and suggesting a positive effect of T1AM upon the steady-state mitochondrial energy production. Such an activating effect is ascribed to IF_1 release from F_0F_1-ATP synthase and is consistent with that obtained by IF_1-stripping treatment (alkaline pH and high saline concentrations) of mitochondria isolated from this cell line (Comelli *et al.*, 2007). *In vivo* activation, corresponding to an increase in ATP synthase molecules available for synthesis, was previously reported as being related to IF_1 release by different triggers, such as electrical stimulation of cardiomyocytes (Das and Harris, 1990) and cardiac reactive hyperaemia (Di Pancrazio *et al.*, 2004; Penna *et al.*, 2004). It should be noted that the IF_1 content in H9c2 cells was estimated to be around 2 μM, which is not far from data reported by Giorgio *et al.* (2010) and is well in excess of the T1AM concentration in our experiments (around 50 nM). It was thus likely that T1AM can be concentrated inside H9c2 mitochondria, as found for cells (Saba *et al.*, 2010). The subcellular distribution of T1AM remains to be clarified and it is possible that its concentration in specific compartments such as mitochondria may be significantly different from the average concentrations that have been measured so far (Saba *et al.*, 2010; Zucchi *et al.*, 2010). In conclusion, in the light of our data, endogenous T1AM levels may be able to contribute to the regulation of the steady-state binding of IF_1 to F_0F_1-ATP synthase. Of note, based on the low level of bound IF_1 observed in H9c2 cardiomyocytes (Comelli *et al.*, 2007) and the correlation with heart rate (Rouslin *et al.*, 1995), a more pronounced effect may be expected in low heart rate mammalian species containing high IF_1 levels (Rouslin *et al.*, 1995; Di Pancrazio *et al.*, 2004). Nevertheless, the physiological implications of our findings require further investigations.

It is not clear whether the inhibitory effect of T1AM upon ATP synthase activity which requires micromolar concentrations, would have a physiopathological or pharmacological role. Nevertheless, some systemic effects of T1AM have been reported to occur at micromolar concentrations (Chiellini *et al.*, 2007), which could correspond to putative therapeutic doses of T1AM. Of note, there is convincing evidence that down-modulation of ATP synthase afforded by the benzodiazepine derivative Bz-423 results in selective killing of autoimmune lymphocytes and alloreactive T cells through activation of apoptotic signalling (Gatza *et al.*, 2011; Johnson and Ogbi, 2011). Designing a pharmacological strategy to target the ATP synthase with a natural compound such as T1AM may extend the reange of therapies for autoimmune and immune disorders.

The potential beneficial contribution of ATP synthase inhibition to the protection of the ischemic heart by T1AM appears to be counterintuitive and needs obviously further *ad hoc* investigation. Distinct mechanisms may be involved in T1AM cardioprotection, and they have only partially been

elucidated, although pharmacological evidence suggests a potential role of mitochondrial effects (Frascarelli *et al.*, 2011). In principle, T1AM treatment may transiently limit ATP synthesis at the onset of reperfusion, when an increase in ATP concentration occurs and paradoxically contributes to reperfusion injury, leading to hyper-contracture of cardiomyocytes, membrane disruption and subsequent necrosis (Piper *et al.*, 2004). Thus, T1AM may reduce the risk of developing myocardial hypercontracture, which seems to be a major mechanism of early reperfusion-induced cell death. However, excessive inhibition of ATP synthesis would obviously be detrimental. Therefore, T1AM administration should be carried out after thorough consideration of the relevant potential side effects linked to excessive energy impairment. On the other hand, it should call attention to a paradoxical effect that may be elicited on F_0F_1-ATP synthase working in ATPase-mode in the ischemic heart by T1AM-mediated IF_1 release, if any. It is relevant to note that in states of compromised ATP production, such as prolonged ischemia, IF_1 may lose effectiveness because reduced ATP and supraphysiological levels of Ca^{2+} and Mg^{2+} favour IF_1 release from F_0F_1-ATP synthase, thereby suppressing the energy–sparing, endogenous, protective mechanism. Under such conditions, in which ATP hydrolysis prevails, the inhibitory effects of T1AM may be more relevant, as shown *in vitro* on IF_1-free ASp, and represent an alternative mechanism for minimizing ATP loss.

Finally, the use of T1AM as an F_0F_1-ATP synthase-directed agent might have some side-effects. There is now convincing evidence that T1AM is a chemical messenger with widespread effects, ranging from metabolic regulation to neuromodulation, to the control of insulin and glucagon secretion, and possibly to behavioural effects. Therefore, administration of exogenous T1AM, or interference with T1AM metabolism, should be carried out with great care.

Acknowledgements

This work was supported by the Italian Ministero dell'Università e della Ricerca Scientifica (MIUR), through grants PRIN 2007 and the Italian Human ProteomeNet Project (FIRB 2006). We thank Dr F. Haraux (Service de Bioénergétique, Biologie Structurale et Mécanismes and CNRS-URA 2096, iBiTec-S, CEA Saclay, F 91191 Gif-sur-Yvette, France) for his helpful discussions.

Conflicts of interest

The authors declare no conflicts of interest.

References

Abrahams JP, Leslie AJ, Lutter R, Walker JE (1994). Structure at 2.8 A resolution of F_1-ATPase from bovine heart mitochondria. Nature 370: 621–628.

Alexander SPH, Mathie A, Peters JA (2011). Guide to Receptors and Channels (GRAC), 5th Edition. Br J Pharmacol 164 (Suppl. 1): S1–S324.

Bason JV, Runswick MJ, Fearnley IM, Walker JE (2011). Binding of the inhibitor protein IF(1) to bovine F(1)-ATPase. J Mol Biol 406: 443–453.

Bertina RM, Schrier PI, Slater EC (1973). The binding of aurovertin to mitochondria, and its effect on mitochondrial respiration. Biochim Biophys Acta 305: 503–518.

Boyer PD (1997). The ATP synthase – a splendid molecular machine. Annu Rev Biochem 66: 717–749.

Braulke LJ, Klingenspor M, DeBarber A, Tobias SC, Grandy DK, Scanlan TS *et al.* (2008). 3-Iodothyronamine: a novel hormone controlling the balance between glucose and lipid utilisation. J Comp Physiol B 178: 167–177.

Bullough DA, Ceccarelli EA, Roise D, Allison WS (1989). Inhibition of the bovine-heart mitochondrial F_1-ATPase by cationic dyes and amphipathic peptides. Biochim Biophys Acta 975: 377–383.

Cabezon E, Montgomery MG, Leslie AG, Walker JE (2003). The structure of bovine F_1-ATPase in complex with its regulatory protein IF_1. Nat Struct Biol 10: 44–750.

Campanella M, Casswell E, Chong S, Farah Z, Wieckowski MR, Abramov AY *et al.* (2008). Regulation of mitochondrial structure and function by the F_1F_0-ATPase inhibitor protein, IF_1. Cell Metab 8: 13–25.

Campanella M, Seraphim A, Abeti R, Casswell E, Echave P, Duchen MR (2009). IF_1, the endogenous regulator of the F(1)F(o)-ATP synthase, defines mitochondrial volume fraction in HeLa cells by regulating autophagy. Biochim Biophys Acta 1787: 393–401.

Capaldi RA, Aggeler R (2002). Mechanism of the F(1)F(0)-type ATP synthase, a biological rotary motor. Trends Biochem Sci 27: 154–160.

Champagne E, Martinez LO, Collet X, Barbaras R (2006). Ecto- F_0F_1 ATP synthase/F_1 ATPase: metabolic and immunological functions (review). Curr Opin Lipidol 17: 279–284.

Chiellini G, Frascarelli S, Ghelardoni S, Carnicelli V, Tobias SC, DeBarber A *et al.* (2007). Cardiac effects of 3-iodothyronamine: a new aminergic system modulating cardiac function. FASEB J 21: 1597–1608.

Cole ST, Alzari PM (2005). Microbiology. TB-a new target, a new drug. Science 307: 223–227.

Comelli M, Metelli G, Mavelli I (2007). Downmodulation of mitochondrial F_0F_1 ATP synthase by diazoxide in cardiac myoblasts: a dual effect of the drug. Am J Physiol Heart Circ Physiol 292: H820–H829.

Comelli M, Domenis R, Bisetto E, Contin M, Marchini M, Ortolani F *et al.* (2011). Cardiac differentiation promotes mitochondria development and ameliorates oxidative capacity in H9c2 cardiomyoblasts. Mitochondrion 11: 315–326.

Contessi S, Metelli G, Mavelli I, Lippe G (2004). Diazoxide affects the IF_1 inhibitor protein binding to F_1 sector of beef heart F_0F_1ATP synthase. Biochem Pharmacol 67: 1843–1851.

Contessi S, Comelli M, Cmet S, Lippe G, Mavelli I (2007). F_1 distribution in HepG2 cells in relation to ecto– F_0F_1ATP synthase and calmodulin. J Bioenerg Biomembr 39: 291–300.

Cross RL, Kohlbrenner WE (1978). The mode of inhibition of oxidative phosphorylation by efrapeptin (A23871). Evidence for an alternating site mechanism for ATP synthesis. J Biol Chem 253: 4865–4873.

Das AM, Harris DA (1990). Regulation of the mitochondrial ATP synthase in intact rat cardiomyocytes. Biochem J 266: 355–361.

Di Pancrazio F, Mavelli I, Isola M, Losano G, Pagliaro P, Harris DA *et al.* (2004). In vitro and in vivo studies of F_0F_1-ATP synthase regulation by inhibitor protein IF_1 in goat heart. Biochim Biophys Acta 1659: 52–62.

Dickson VK, Silvester JA, Fearnley IM, Leslie AG, Walker JE (2006). On the structure of the stator of the mitochondrial ATP synthase. EMBO J 25: 2911–2918.

Ferguson SJ, Harris DA, Radda OK (1977). The adenosine triphosphataseinhibitor content of bovine heart submitochondrial particles. Influence of the inhibitor on adenosine triphosphate-dependent reactions. Biochem J 162: 351–357.

Frascarelli S, Ghelardoni S, Chiellini G, Galli E, Ronca F, Scanlan TS *et al.* (2011). Cardioprotective effect of 3-iodothyronamine in perfused rat heart subjected to ischemia and reperfusion. Cardiovasc Drugs Ther 25: 307–313.

Galli E, Marchini M, Saba A, Berti S, Tonacchera M, Vitti P *et al.* (2012). Detection of 3-Iodothyronamine in human patients: a preliminary study. J Clin Endocrinol Metab 97: E69–E74.

García JJ, Morales-Ríos E, Cortés-Hernandez P, Rodríguez-Zavala JS (2006). The inhibitor protein (IF_1) promotes dimerization of the mitochondrial F_1F_0-ATP synthase. Biochemistry 45: 12695–12703.

Gatza E, Wahl DR, Opipari AW, Sundberg TB, Reddy P, Liu C *et al.* (2011). Manipulating the bioenergetics of alloreactive T cells causes their selective apoptosis and arrests graft-versus-host disease. Sci Transl Med 3: 67ra8.

Ghelardoni S, Suffredini S, Frascarelli S, Brogioni S, Chiellini G, Ronca-Testoni S *et al.* (2009). Modulation of cardiac ionic homeostasis by 3-iodothyronamine. J Cell Mol Med 13: 3082–3090.

Gibbons C, Montgomery MG, Leslie AG, Walker JE (2000). The structure of the central stalk in bovine F_1-ATPase at 2.4A° resolution. Nat Struct Biol 7: 1055–1061.

Giorgio V, Bisetto E, Franca R, Harris DA, Passamonti S, Lippe G (2010). The ectopic F(O)F(1) ATP synthase of rat liver is modulated in acute cholestasis by the inhibitor protein IF1. J Bioenerg Biomembr 42: 117–123.

Gledhill JR, Walker JE (2005). Inhibition sites in F_1-ATPase from bovine heart mitochondria. Biochem J 386: 591–598.

Gledhill JR, Montgomery MG, Leslie AG, Walker JE (2007a). Mechanism of inhibition of bovine F_1-ATPase by resveratrol and related polyphenols. Proc Natl Acad Sci USA 104: 13632–13637.

Gledhill JR, Montgomery MG, Leslie AGW, Walker JE (2007b). How the regulatory protein, IF_1, inhibits F_1-ATPase from bovine mitochondria. Proc Natl Acad Sci USA 104: 15671–15676.

Gnaiger E (2009). Capacity of oxidative phosphorylation in human skeletal muscle. New perspectives of mitochondrial physiology. Int J Biochem Cell Biol 41: 1837–1845.

Gomez-Fernandez JC, Harris DA (1978). A thermodynamic analysis of the interaction between the mitochondrial coupling adenosine triphosphatase and its naturally occurring inhibitor protein. Biochem J 176: 967–975.

Grandy DK (2007). Trace amine-associated receptor 1-Family archetype or iconoclast? J Pharmacol Ther 116: 355–390.

Green DW, Grover GJ (2000). The IF_1 inhibitor protein of the mitochondrial F_0F_1-ATPase. Biochim Biophys Acta 1458: 343–355.

Grover GJ, Malm J (2008). Pharmacological profile of the selective mitochondrial F_1F_0-ATP hydrolase inhibitor BMS-199264 in myocardial ischemia (Review). Cardiovasc Ther 26: 287–295.

Grover GJ, Atwal KS, Sleph PG, Wang FL, Monshizadegan H, Monticello T *et al.* (2006). Excessive ATP hydrolysis in ischemic myocardium by mitochondrial F_1F_0-ATPase: effect of selective pharmacological inhibition of mitochondrial ATPase hydrolase activity. Am J Physiol Heart Circ Physiol 291: H484.

Hall AM, Unwin RJ, Parker N, Duchen MR (2009). Multiphoton Imaging Reveals Differences in Mitochondrial Function between Nephron Segments. J Am Soc Nephrol 20: 1293–1302.

Harris DA, Das AM (1991). Control of mitochondrial ATP synthesis in the heart. Biochem J 280: 561–573.

Hassinen IE, Vourinen KH, Ylitalo K, Ala-Raämi A (1998). Role of cellular energetics in ischemia–reperfusion and ischemic preconditioning of myocardium. Mol Cell Biochem 184: 393–400.

Hong S, Pedersen L (2008). ATP synthase and the actions of inhibitors utilized to study its roles in human health, disease, and other scientific areas. Microbiol Mol Biol Rev 72: 590–641.

Horstman LL, Racker E (1970). Partial resolution of the enzyme catalyzing oxidative phosphorylation. XXII. Interaction between mitochondrial adenosine triphosphatase inhibitor and mitochondrial adenosine triphosphatase. J Biol Chem 245: 1336–1344.

Ianculescu AG, Scanlan TS (2010). 3-Iothyronamine (T1AM): a new chapter of thyroid hormone endocrinology? Mol Bio Syst 6: 1338–1344.

Ianculescu AG, Giacomini KM, Scanlan TS (2009). Identification and characterization of 3-iodothyronamine intracellular transport. Endocrinology 150: 1991–1999.

Johnson JA, Ogbi M (2011). Targeting the F1Fo ATP synthase: modulation of the body's powerhouse and its implications for human disease. Curr Med Chem 18: 4684–4714.

Johnson KM, Swenson L, Opipari AW Jr, Reuter R, Zarrabi N, Fierke CA *et al.* (2009). Mechanistic basis for differential inhibition of the F_0F_1-ATPase by aurovertin. Biopolymers 91: 830–840.

Kagawa R, Montgomery MG, Braig K, Leslie AG, Walker JE (2004). The structure of bovine F_1-ATPase inhibited by ADP and beryllium fluoride. EMBO J 23: 2734–2744.

Klieverik LP, Foppen E, Ackermans MT, Serlie MJ, Sauerwein HP, Scanlan TS *et al.* (2009). Central effects of thyronamines on glucose metabolism in rats. J Endocrinol 201: 377–386.

Laemmli UK (1970). Cleavage of structural proteins during the assembly of the head of bacteriophage T4. Nature 227: 680–685.

Lee C, Ernster L (1968). Studies of the energy-transfer system of submitochondrial particles. 2. Effects of oligomycin and aurovertin. Eur J Biochem 3: 391–400.

Lenaz G (1965). Effect of aurovertin on energy-linked processes related to oxidative phosphorylation. Biochem Biophys Res Commun 21: 170–175.

Leyva JA, Bianchet MA, Amzel LM (2003). Understanding ATP synthesis: structure and mechanism of the F_1-ATPase. Mol Membr Biol 20: 27–33.

Lippe G, Sorgato MC, Harris DA (1988). The binding and release of the inhibitor protein are governed independently by ATP and membrane potential in ox-heart submitochondrial vesicles. Biochim Biophys Acta 933: 12–21.

Lippe G, Bisetto E, Comelli M, Contessi S, Di Pancrazio F, Mavelli I (2009). Mitochondrial and cell surface F_0F_1ATP synthase in innate and acquired cardioprotection (Review). J Bioenerg Biomembr 41: 151–157.

Lowry OH, Rosenbrough NJ, Far AL, Randall RJ (1951). Protein measurement with Folin phenol reagents. J Biol Chem 193: 265–275.

Martinez-Irujo JJ, Villahermosa ML, Mercapide J, Cabodevilla JF, Santiago E (1998). Analysis of the combined effect of two linear inhibitors on a single enzyme. Biochem J 329: 689–698.

Menz RI, Walker JE, Leslie AG (2001). Structure of bovine mitochondrial F(1)-ATPase with nucleotide bound to all three catalytic sites: implications for the mechanism of rotary catalysis. Cell 106: 331–341.

Morris GM, Huey R, Lindstrom W, Sanner MF, Belew RK, Goodsell DS *et al.* (2009). AutoDock4 and AutoDockTools4: automated docking with selective receptor flexibility. J Comput Chem 30: 2785–2791.

Pedersen PL (2007). Transport ATPases into the year 2008: a brief overview related to types, structures, functions and roles in health and disease. J Bioenerg Biomembr 39: 349–355.

Penna C, Pagliaro P, Rastaldo R, Di Pancrazio F, Lippe G, Gattullo D *et al.* (2004). F_0F_1 ATP synthase activity is differently modulated by coronary reactive hyperemia before and after ischemic preconditioning in the goat. Am J Physiol Heart Circ Physiol 287: H2192–H2200.

Piehl S, Hoefig C, Scanlan TS, Köhrle J (2011). Thyronamines – past, present, and future. Endocr Rev 32: 64–80.

Piper HM, Abdallah Y, Schäfer C (2004). The first minutes of reperfusion: a window of opportunity for cardioprotection. Cardiovasc Res 61: 365–371.

Pirola L, Frojdo S (2008). Resveratrol: one molecule, many targets. IUBMB Life 60: 323–332.

Rees MR, Leslie AGW, Walker JE (2009). The structure of the membrane extrinsic region of bovine ATP synthase. Proc Natl Acad Sci USA 106: 21597–21601.

Regard JB, Kataoka H, Cano DA, Camerer E, Yin L, Zheng YW *et al.* (2007). Probing cell type-specific functions of Gi in vivo identifies GPCR regulators of insulin secretion. J Clin Invest 117: 4034–4043.

Roberton AM, Holloway CT, Knight IG, Beechey RB (1968). A comparison of the effects of NN′-dicyclohexylcarbodi-imide, oligomycin A and aurovertin on enrgy-linked reactions in mitochondria and submitochondrial particles. Biochem J 108: 445–456.

Rouslin W (1983). Protonic inhibition of the mitochondrial oligomycin-sensitive adenosine 50-triphosphatase in ischemic and autolyzing cardiac muscle. Possible mechanism for the mitigation of ATP hydrolysis under nonenergizing conditions. J Biol Chem 258: 9657–9661.

Rouslin W, Broge CW, Guerrieri F, Capozza G (1995). ATPase activity, IF_1 content, and proton conductivity of ESMP from control and ischemic slow and fast heart-rate hearts. J Bioenerg Biomembr 27: 459–466.

Saba A, Chiellini G, Frascarelli S, Marchini M, Ghelardoni S, Raffaelli A *et al.* (2010). Tissue distribution and cardiac metabolism of 3-iodothyronamine. Endocrinology 151: 5063–5073.

Scanlan TS, Suchland KL, Hart ME, Chiellini G, Huang Y, Kruzich PJ *et al.* (2004). 3 iodothyronamine is an endogenous and rapid-acting derivative of thyroid hormone. Nat Med 10: 638–642.

Smith PK, Krohn RI, Hermanson GT, Mallia AK, Gartner FH, Provenzano MD *et al.* (1985). Measurement of protein using bicinchoninic acid. Anal Biochem 150: 76–85.

Snead AN, Santos MS, Seal RP, Miyakawa M, Edwards MH, Scanlan TS (2007). Thyronamines inhibit plasma membrane and vescicular monoamine transport. ACS Chem Biol 2: 390–398.

Stock D, Gibbons C, Arechaga I, Leslie AG, Walker JE (2000). The rotary mechanism of ATP synthase. Curr Opin Struct Biol 10: 672–679.

Tomasetig L, Di Pancrazio F, Harris DA, Mavelli I, Lippe G (2002). Dimerization of F_0F_1ATP synthase from bovine heart is independent from the binding of the inhibitor protein IF_1. Biochim Biophys Acta 1556: 133–141.

Trott O, Olson AJ (2010). AutoDock Vina: improving the speed and accuracy of docking with a new scoring function, efficient optimization, and multithreading. J Comput Chem 31: 455–461.

Vadineanu A, Berden JA, Slater EC (1976). Proteins required for the binding of mitochondrial ATPase to the mitochondrial inner membrane. Biochim Biophys Acta 449: 468–479.

Van Raaij MJ, Abrahams JP, Leslie AG, Walker JE (1996). The structure of bovine F_1-ATPase complexed with the antibiotic inhibitor aurovertin B. Proc Natl Acad Sci USA 93: 6913–6917.

Venditti P, Napolitano G, Di Stefano L, Chiellini G, Zucchi R, Scanlan TS *et al.* (2011). Effects of the thyroid hormone derivatives 3-iodothyronamine and thyronamine on rat liver oxidative capacity. Mol Cell Endocrinol 341: 55–62.

Watt IN, Montgomery MG, Runswick MJ, Leslie AG, Walker JE (2010). Bioenergetic cost of making an adenosine triphosphate molecule in animal mitochondria. Proc Natl Acad Sci USA 107: 16823–16827.

Yonetani T, Theorell H (1964). Studies on liver alcohol hydrogenase complexes. III. Multiple inhibition kinetics in the presence of two competitive inhibitors. Arch Biochem Biophys 106: 243–251.

Zheng J, Ramirez VD (1999). Piceatannol, a stilbene phytochemical, inhibits mitochondrial F_0F_1-ATPase activity by targeting the F_1 complex. Biochem Biophys Res Commun 261: 499–503.

Zheng J, Ramirez VD (2000). Inhibition of mitochondrial proton F_0F_1-ATPase/ATP synthase by polyphenolic phytochemicals. Br J Pharmacol 130: 1115–1123.

Zucchi R, Chiellini G, Scanlan TS, Grandy DK (2006). Trace amine-associated receptors and their ligands. Br J Pharmacol 149: 967–978.

Zucchi R, Ghelardoni S, Chiellini G (2010). Cardiac effects of thyronamines. Heart Fail Rev 15: 171–176.

Supporting information

Additional Supporting Information may be found in the online version of this article:

Figure S1 Quantification of IF_1 in ASp, type II SMP and type I SMP.
Figure S2 T1AM and resveratrol inhibition mechanism in F_1-ATPase.
Figure S3 Immunodetection of IF_1 in H9c2 cells by quantitative Western blot analysis.

Please note: Wiley-Blackwell are not responsible for the content or functionality of any supporting materials supplied by the authors. Any queries (other than missing material) should be directed to the corresponding author for the article.